Article

Development of a conformational histamine H receptor biosensor for the synchronous screening of agonists and inverse agonists.

Hannes Schihada, Xiaoyuan Ma, Ulrike Zabel, Henry F. Vischer, Gunnar Schulte, Rob Leurs, Steffen Pockes, and Martin J. Lohse

ACS Sens., **Just Accepted Manuscript** • DOI: 10.1021/acssensors.0c00397 • Publication Date (Web): 13 May 2020

Development of a conformational histamine H_3 receptor biosensor for the synchronous screening of agonists and inverse agonists.

Hannes Schihada[1,2] *, Xiaoyuan Ma[3], Ulrike Zabel[2], Henry F. Vischer[3], Gunnar Schulte[1], Rob Leurs[3], Steffen Pockes[4], Martin J. Lohse[2,5] *

[1]: Section of Receptor Biology & Signaling, Dept. Physiology & Pharmacology, Karolinska Institutet, Stockholm, Sweden.
[2]: Institute of Pharmacology and Toxicology and Rudolf Virchow Center, University of Würzburg, Würzburg, Germany
[3]: Amsterdam Institute for Molecules, Medicines and Systems, Division of Medicinal Chemistry, Faculty of Science, Vrije Universiteit Amsterdam, Amsterdam, The Netherlands.
[4]: Institute of Pharmacy, Faculty of Chemistry and Pharmacy, University of Regensburg, Regensburg, Germany.
[5]: ISAR Bioscience, Planegg, Germany

KEYWORDS: *GPCR, BRET, conformational sensor, histamine receptor, inverse agonist, drug discovery*

ABSTRACT: The histamine H_3 receptor (H_3R) represents a highly attractive drug target for the treatment of various central nervous disorders but the discovery of novel H_3R targeting compounds relies on the assessment of highly amplified intracellular signaling events that do not only reflect H_3R modulation and carry the risk of high false-positive and -negative screening rates. To address these limitations, we designed an intramolecular H_3R biosensor based on the principle of bioluminescence-resonance-energy-transfer (BRET) that reports the receptor's real-time conformational dynamics and provides an advanced tool to screen for both, H_3R agonists and inverse agonists in a live cell screening-compatible assay format. This conformational G-protein-coupled receptor (GPCR) sensor allowed us to characterize the pharmacological properties of known and new H_3 receptor ligands with unprecedented accuracy. Intriguingly, we found that one newly developed H_3 receptor ligand possesses even stronger inverse agonistic activity than reference H_3R inverse agonists including the current gold standard pitolisant. Taken together, we describe here the design and validation of the first screening-compatible H_3R conformational biosensor that will aid in the discovery of novel H_3R ligands and can be employed to gain deeper insights into the (in-)activation mechanism of this highly attractive drug target.

The group of histamine receptors belongs to the superfamily of G-protein-coupled receptors (GPCRs) and comprises four distinct subtypes named H_1, H_2, H_3 and H_4 receptor ($H_{1\text{-}4}R$) that are of highest interest for modern drug discovery.[1] First H_1R and H_2R antagonists were already developed in the 1930s and 1970s, respectively, leading to the extensive medical use of numerous antiallergic and antiulcer pharmaceutics including loratadine (H_1R) and ranitidine (H_2R) that are listed in the WHO register of essential medicines.[2, 3]

Likewise, the discovery of the subtype H_3R has raised intense hopes for the development of similarly successful drugs.[4] In humans, the H_3R is almost exclusively expressed in the central nervous system (CNS) and considered to work both, as an autoreceptor in presynaptic membranes and as a postsynaptic heteroreceptor controlling the release of other neurotransmitters including acetylcholine, norepinephrine and dopamine.[5] Therefore, pharmacological modulation of the H_3R represents an attractive approach to treat various central nervous diseases such as Parkinson's, Huntington's and Alzheimer's disease and tic disorders.[1, 6-9] In addition, pitolisant, an H_3R inverse agonist that reduces the basal signalling capacity of the receptor (known as receptor constitutive activity), has entered the market four years ago for the treatment of narcolepsia.[10] Despite increasing efforts to develop novel H_3R modulating compounds,[11-17] thus far, pitolisant represents the only H_3R ligand that is approved by health authorities. This is partially due to the limited power of our current screening technologies that are mainly based on receptor downstream signalling events. For instance, measuring compound-induced β-arrestin translocation is one of the most common assays employed in GPCR drug discovery campaigns. However, this approach not only fails to detect G-protein-biased H_3R agonists but also misses receptor inverse agonists like pitolisant. Identification of pitolisant with such a setup would instead require preincubation with selective H_3R agonists but, in turn, hamper the discovery of H_3R receptor agonists.

In contrast to these signalling dependent assays, downstream-independent screening methods that detect ligands with distinct efficacies (e.g. agonists vs. inverse agonists) and specific downstream signalling profiles (e.g. G-protein-biased vs. β-arrestin-biased agonists) would allow for the simultaneous screening of compounds with differing pharmacological profiles and thus, are highly desired to speed up the discovery of novel GPCR ligands.

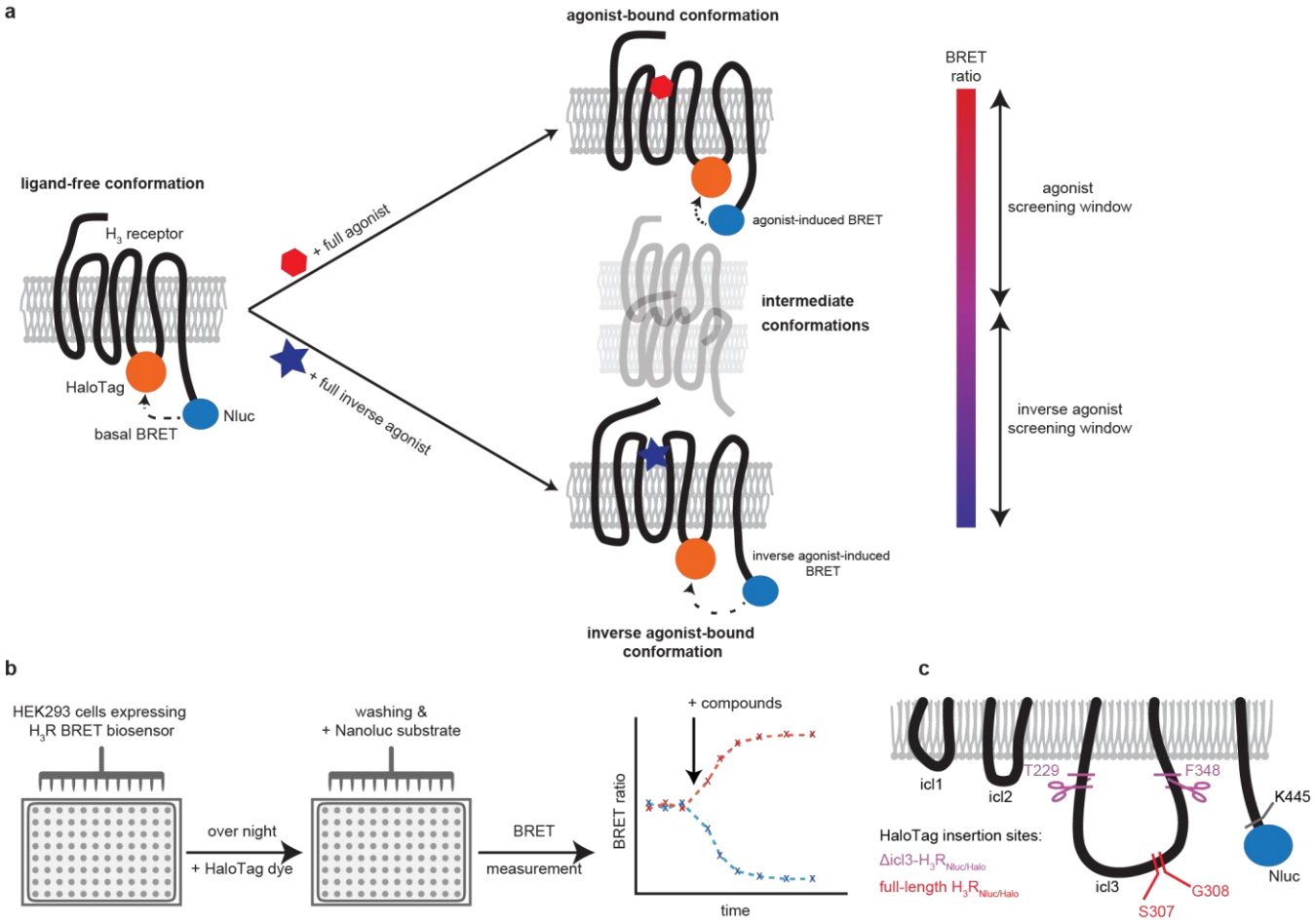

Scheme 1. Principle of the sensor and assay design. a) The BRET partners HaloTag and Nluc are fused to the third intracellular loop and C-terminus of the histamine H_3 receptor, respectively. The proximity of the BRET patners allows for energy transfer from the donor Nluc to HaloTag. Upon binding of full agonists or full inverse agonists, the receptor undergoes conformational changes to the fully active (bottom right) or inactive (top right) state affecting the efficiency of energy transfer. b) Assay protocol. c) Insertion sites of Nluc and HaloTag in two H_3R biosensor versions.

Conformational GPCR biosensors based on fluorescence and bioluminescence resonance energy transfer (FRET, BRET) have proven valuable tools to determine the pharmacological profiles of GPCR ligands in a real-time and live cell assay system.[18] Since the receptor's conformational change follows directly upon ligand binding without any signal amplification, this approach represents the most undistorted way to assess ligand efficacy and potency; as a consequence, these conformational readouts reveal differences among distinct test compounds where downstream-dependent assays report indiscernible activities.[19-21] Furthermore, single-cell studies employing FRET-based conformational biosensors of H_1R and H_3R have recently provided precious insights into the mechano-sensing mechanism and the activation kinetics of histamine receptors, respectively.[22, 23] Recently, the suitability of such sensors for high-throughput screening has been demonstrated by employing a novel BRET system composed of the small engineered luciferase NanoLuciferase (Nluc)[24] and a red fluorescent HaloTag dye[25], as demonstrated for two class A (α_{2A}-adrenergic and β_2-adrenergic receptor) and one class B GPCR (parathyroid hormone receptor 1).[19]

In this study, we set out to address the urgent need for a downstream-independent and very sensitive screening platform for the highly attractive drug target, the H_3R. By fusing the BRET partners Nluc and HaloTag to this histamine receptor subtype, we generate a conformational biosensor that enables the simultaneous detection of agonists and inverse agonists with screening-compatible assay sensitivity. Furthermore, using this biosensor, we characterized pharmacologically in addition to several well-known H_3R standard ligands two novel H_3R inverse agonists, that have recently been identified in a virtual screening campaign.[26] We show that one of these ligands possesses even stronger inverse agonistic activity than pitolisant and reduces H_3R-mediated G_i-protein activity with nanomolar potencies.

Experimental Section

Plasmids

Wildtype human H_3R DNA (GeneID 11255) in pcDNA3.1 vector was purchased from cDNA.org. Nluc was fused at position K445 to generate C-terminally tagged H_3R_{Nluc}. Thereafter,

a HaloTag was inserted between S307 / G308 (full-length $H_3R_{Nluc/Halo(618)}$) or between T229 / F348 (Δicl3-$H_3R_{Nluc/Halo(618)}$) within the third intracellular loop of H_3R_{Nluc}. All cloning steps were performed using established PCR strategies and restriction enzymes and constructs were verified by sequencing (Eurofins genomics). Plasmids encoding tagged and native G-protein subunits were kindly provided by A. Inoue (Tohoku University, Sendai, Japan).

Reagents

Histamine dihydrochloride, imetit dihydrobromide, clobenpropit dihydrobromide, thioperamide and pitolisant (BF 2649 hydrochloride) were purchased from Tocris Bioscience (Wiesbaden-Nordenstadt, Germany). Poly-D-lysine and geneticin were obtained from Sigma Aldrich (Taufkirchen, Germany). [^{3}H]NAMH (specific activity: 79.7 Ci/mmol) was from PerkinElmer (Waltham, MA, USA). Z27743747 and Z3303614736 were purchased from Enamine Ltd (Kyiv, Ukraine). The Nluc substrate furimazine and the HaloTag fluorescent dye NanoBRET 618 were obtained from Promega (Madison, WI, USA). UR-PI294, VUF4903, VUF4904 and VUF5207 were synthesized as described previously.[27, 28] White-wall, white-bottomed 96-well microtiter plates were from Brand (Wertheim, Germany) and Gibco (Waltham, MA, USA).

Cell culture

HEK293T and HEK293A cells were used for transient expression of GPCR and G-protein biosensors and grown in Dulbecco's Modified Eagle's Medium (DMEM) supplemented with 2 mM glutamine, 10% fetal calf serum, 0.1 mg/mL streptomycin, and 100 units/mL penicillin at 37 °C with 5% CO_2. To generate the cell line stably expressing Δicl3-$H_3R_{Nluc/Halo(618)}$, HEK293A cells grown in T75 flasks were transfected at a confluence of 50 % with 1 µg DNA using Lipofectamine 2000 (Thermo Fisher Scientific, Waltham, MA, USA). Stably transfected cells were selected with 2 mg/mL geneticin and maintained in supplemented DMEM containing 500 µg/mL geneticin.

Radioligand binding

HEK293A cells stably expressing Δicl3-$H_3R_{Nluc/Halo(618)}$ or HEK293T cells transiently transfected with 2.5 µg wildtype H_3R cDNA grown in 10 cm^2 culture dishes were collected (48 hours after transfection for wildtype H_3R) in cold phosphate-buffered saline (PBS) and centrifuged at 3,000 g for 15 minutes at 4°C. Supernatant was discarded and the cell pellet was stored at −20°C until the day of the experiment. Prior to the experiment, cell pellets (200 µg/ml) were resuspended in binding buffer (50 mM Tris-HCl, pH 7.4) and disrupted using a Branson sonifier 250 (Boom B.V., Meppel, The Netherlands).

For saturation binding, 50 µl of cell pellets were incubated with increasing concentrations of [^{3}H]NAMH for 2 hours at 25°C. Nonspecific binding was measured in the presence of 100 µM histamine. Equilibrium competition binding was assayed on 50 µl of cell homogenates with 2 nM [^{3}H]NAMH in the absence and presence of increasing concentrations of unlabelled ligands for 2 hours at 25°C. To terminate incubation, homogenates were filtered over a 0.5% PEI-coated 96-well GF/C filter plate using a PerkinElmer 96-well Filtermate-harvester. After three rapid wash steps with ice-cold binding buffer, the GF/C filter plates were dried at 55°C. Subsequently, 25 µl of Microscint-O scintillation liquid (PerkinElmer, Groningen, The Netherlands) was added per well and incubated for 2 hours to quantify filter-bound radioactivity using a Microbeta Wallac Trilux scintillation counter (PerkinElmer).

Transient transfection and plating

The day before transient transfection, 1.5 × 10^6 HEK293T (for G-protein experiments) or HEK293A cells (for H_3R conformational sensors) were seeded in T25 flasks. The next day, 1 µg of pcDNA3.1 plasmid encoding either of the two H_3R biosensors was transfected using Lipofectamine 2000. For G-protein experiments, cells were transfected with 200 ng LargeBit-$G_{\alpha i1}$, 1 µg $G_{\beta 5}$-smallBit, 1 µg $G_{\gamma 2}$ and 400 ng wildtype H_3R plasmids. Twenty-four hours after transfection, cells were resuspended in supplemented DMEM, mixed with 50 nM HaloTag NanoBret 618 if H_3R conformational biosensors were transfected, and transferred to poly-D-lysine pre-coated white 96-well plates at a density of 50,000 cells per well.

Recording of BRET emission spectra

HEK293T cells were transfected and labelled as described above. Luminescence emission spectra of H_3R sensors were recorded in HBSS with 4 nm resolution upon addition of 1:1,000 furimazine dilution using a CLARIOstar plate reader (BMG, Ortenberg, Germany). Spectra were normalized to the donor emission peak.

BRET and luminescence measurements

Cells transiently or stably expressing the H_3R biosensors or H_3R wildtype along with native and tagged G-protein subunits were washed with HBSS and incubated with 1/1,000 dilution of furimazine stock solution. After incubation for 3 minutes at 37 °C, the basal BRET ratio (H_3R biosensor) or absolute Nluc luminescence (G-protein) was measured. Subsequently, 10 µL of 10-fold ligand solution or vehicle control was applied per well and the stimulated BRET ratio or luminescence was recorded. All experiments were conducted at 37 °C with a Synergy Neo2 (Biotek, Winooski, VT, USA) or CLARIOstar plate reader. Nluc emission intensity was selected using a 460/40 nm filter (Neo2) or 450/50 nm monochromator (CLARIOstar). For HaloTag NanoBRET 618 a 620/20 nm filter or 620/30 nm monochromator was used. All experiments were conducted with an integration time of 0.3 seconds.

Data analysis and statistics

BRET ratios were defined as acceptor emission / donor emission. Three individual luminescence or BRET values were averaged before and after ligand addition (lum_{basal} and lum_{stim}; $Ratio_{basal}$ and $Ratio_{stim}$, respectively). To quantify ligand-induced changes, Δluminescence (Δlum) and ΔBRET were calculated for each well as a percent over basal ([(lum_{stim}− lum_{basal})/ lum_{basal}] × 100; [($Ratio_{stim}$− $Ratio_{basal}$)/ $Ratio_{basal}$] × 100). Subsequently, the average Δlum / ΔBRET of vehicle control was subtracted. Z-factors were calculated based on the following equation:

$$\mathbf{Z-factor} = \frac{(\mathbf{3\ x\ \sigma}[\boldsymbol{compound}] + \mathbf{3\ x\ \sigma}[\boldsymbol{vehicle}])}{(\boldsymbol{\mu}[\boldsymbol{compound}] - \boldsymbol{\mu}[\boldsymbol{vehicle}])}$$

where σ and µ are the standard deviations and average ΔBRET values of 10 µM histamine and vehicle control, respectively. For Z-factor experiments using pitolisant as a positive control, the denominator in the equation was replaced by "(µ[vehicle]-µ[compound])".

Signal-to-noise (S/N) ratios in the Δicl3-$H_3R_{Nluc/Halo(618)}$ assay were calculated according to the following equation:

$$\boldsymbol{S/N} = \frac{\mathbf{average\ \Delta BRET}[\boldsymbol{vehicle}] - \mathbf{average\ \Delta BRET}[\boldsymbol{compound}]}{\mathbf{standard\ deviation}[\boldsymbol{vehicle}]}$$

S/N ratios in the split Nluc-based G_{i1} assay were calculated according to the following equation:

$$S/N = \frac{\textbf{average } \Delta\textbf{lum}[\boldsymbol{compound}] - \textbf{average } \Delta\textbf{lum}[\boldsymbol{vehicle}]}{\textbf{standard deviation}[\boldsymbol{vehicle}]}$$

Data were analysed using Prism 5.0 software (GraphPad, San Diego, CA, USA). Data from BRET and luminescence concentration–response experiments were fitted using a four-parameter fit. Data from radioligand saturation binding experiments were fitted using a one-site fitting model. Competition-binding curves were fitted to a one-site binding model to obtain the IC_{50} value. Equilibrium dissociation constants (K_i) of unlabelled ligands were subsequently calculated using the Cheng-Prusoff equation:

$$K_i = \frac{IC_{50}}{1 + {[L]}/{K_D}}$$

where [L] is the concentration of labelled ligand, and K_D the equilibrium dissociation constant of the labelled ligand. Statistical differences were assessed by one-way ANOVA followed by Bonferroni multiple comparison or extra-sum-of-squares F test. Differences were considered significant for values of $p < 0.05$.

Results and Discussion

Design and comparison of two H_3R conformational biosensor versions

The development of ligand-sensitive conformational GPCR biosensors often requires the testing of different (i) resonance energy partner combinations, (ii) insertion sites for the FRET and BRET tags or (iii) major modifications of the original receptor sequence.

We have previously shown that the combination of Nluc and HaloTag(618) yields the most sensitive conformational sensors for three model GPCRs[19] and therefore employed this BRET pair to create two distinct variants of conformational $H_3R_{Nluc/Halo}$ biosensors and monitor their conformational dynamics in a 96-well microtiter format (**Scheme 1a**, **b**). To minimize the manipulation of the natural H_3 receptor, we first generated a full-length H_3R sensor version by placing HaloTag between S307 and G308 in the third intracellular loop (icl3) and fusing NanoLuc to the C-terminal amino acid K445 (full-length $H_3R_{Nluc/Halo(618)}$). In some previously published conformational GPCR sensors, a long icl3, as it is also present in H_3R (142 amino acids), has been associated with issues for sensor engineering and was truncated to yield a ligand-sensitive biosensor.[29-31] Thus, in a second approach, we took advantage of a previously validated FRET-based H_3R conformational sensor design that enabled the assessment of H_3R activation kinetics in a single-cell assay format.[23] In compliance with this sensor design, we fused Nluc to K445 and placed HaloTag between amino acids T229 and F348 to generate an analogous BRET H_3R conformational sensor (Δicl3-$H_3R_{Nluc/Halo(618)}$) and monitor ligand-H_3R interaction in a 96-well microtiter format (**Scheme 1c**).[23]

These two sensor constructs were transiently expressed in HEK293 cells to record the luminescence emission spectra upon addition of the Nluc substrate furimazine (**Figure 1a, b**). Both variants displayed the typical Nluc emission maximum around 450 nm and an additional peak at 620 nm. The latter is specific for the BRET acceptor fluorophore HaloTag(618) and indicates resonance energy transfer in the basal ligand-free states of both biosensors. Subsequently, we assessed the ability of these sensor variants to detect the GPCR conformational dynamics upon addition of the well-characterized H_3R ligands histamine (endogenous full agonist), imetit (synthetic full agonist), clobenpropit (inverse agonist) and pitolisant (inverse agonist) (**Chart 1**).

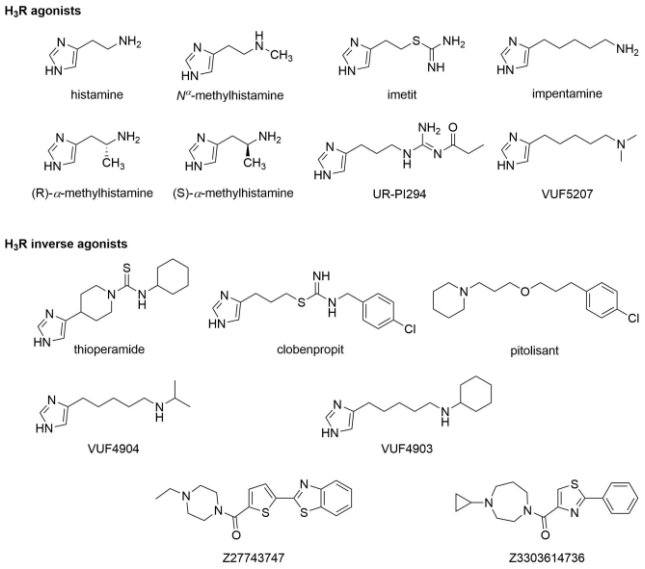

Chart 1. Chemical structures of histamine H_3 receptor agonists and inverse agonists applied in this study.

We incubated HEK293 cells transiently expressing either of the two sensor versions with these reference ligands or vehicle control and recorded the resulting change in BRET over baseline in 96-well microtiter plates. These experiments revealed that full-length $H_3R_{Nluc/Halo(618)}$ does not detect the conformational dynamics of the H_3R since no significant BRET change was observed (**Figure 1c**). In contrast, the BRET ratio of Δicl3-$H_3R_{Nluc/Halo(618)}$ expressing cells increased upon stimulation with the two full agonists histamine and imetit and decreased slightly after addition of the inverse agonist pitolisant (**Figure 1d**).

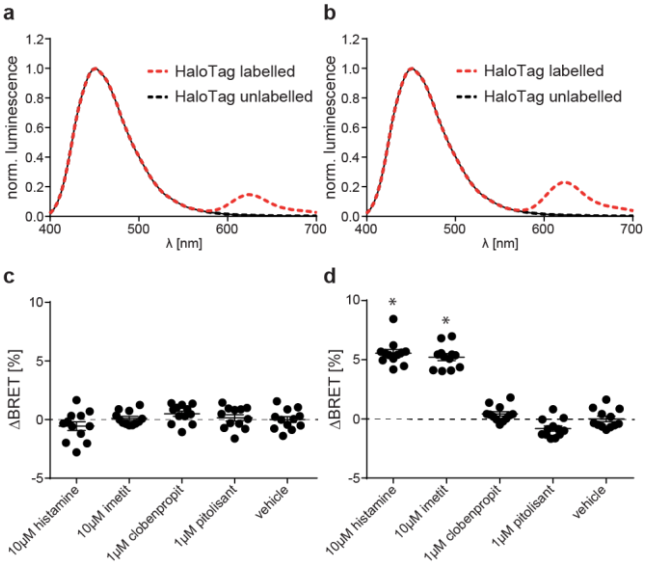

Figure 1. Comparison of two $H_3R_{Nluc/Halo(618)}$ biosensor versions. a, b) Representative luminescence emission spectra of full-length $H_3R_{Nluc/Halo(618)}$ (a) and Δicl3-$H_3R_{Nluc/Halo(618)}$ (b). c, d) BRET changes reported by full-length $H_3R_{Nluc/Halo(618)}$ (c) and Δicl3-

$H_3R_{Nluc/Halo(618)}$ (d) upon addition of H_3R reference ligands. All experiments were conducted in HEK293 cells transiently transfected with the indicated biosensor. Data in c and d show pooled data from three independent experiments. *p < 0.05 vs. vehicle control.

Validation of Δicl3-$H_3R_{Nluc/Halo}$

The Δicl3-$H_3R_{Nluc/Halo(618)}$ biosensor proved capable of detecting the ligand-induced receptor conformational changes in transiently transfected HEK293 cells (**Figure 1d**). To evaluate the ligand binding properties of Δicl3-$H_3R_{Nluc/Halo(618)}$, we next conducted classical radioligand saturation binding experiments. Here, incubation with the radiolabelled H_3R agonist N-α-methylhistamine ([^{3}H]NAMH) saturated with a pK_D of 8.7 ± 0.2 (mean ± s.d.), similar to what we observed with cells expressing wildtype H_3R (pK_D = 8.9 ± 0.1) (**Figure 2a**, **Supplementary Table 1**). In addition, radioligand displacement experiments at Δicl3-$H_3R_{Nluc/Halo(618)}$ with a panel of H_3R reference ligands yielded pK_i-values that were in general accordance with previously published data (**Figure 2b**, **Supplementary Table 1**, **Supplementary Figure 1**). Importantly, Δicl3-$H_3R_{Nluc/Halo(618)}$ maintains the distinct binding affinities for the enantiomers (R)-α-methylhistamine (RAMH) and (S)-α-methylhistamine (SAMH) known from wildtype H_3R. Taken together, these binding experiments reveal that Δicl3-$H_3R_{Nluc/Halo(618)}$, similar to its original FRET analogue[23], possesses wildtype binding properties, which represents a key requirement for its utility in ligand screening campaigns.

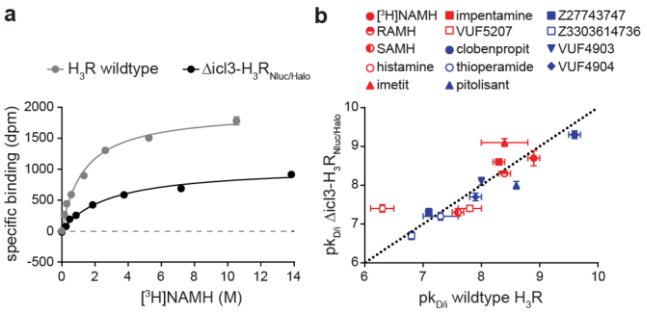

Figure 2. Ligand binding properties of Δicl3-$H_3R_{Nluc/Halo(618)}$. a) Saturation binding of the radiolabelled H_3R agonist [^{3}H]NAMH to wildtype H_3R and Δicl3-$H_3R_{NlucHalo(618)}$. b) Correlation of ligand binding affinities to wildtype H_3R (values extracted from literature except for [^{3}H]NAMH; see also Supplementary Table 1) and Δicl3-$H_3R_{NlucHalo(618)}$ (red: agonists; blue: inverse agonists). Dotted line indicates line of unity. Experiments were conducted using membranes from transiently (a) or stably expressing (b) HEK293 cells. Data show mean ± s.e.m. of one representative (a) or at least three independent experiments (b).

In order to improve the assay's dynamic range, we next generated a HEK293 cell line stably expressing Δicl3-$H_3R_{Nluc/Halo(618)}$ and conducted live cell BRET experiments to demonstrate its suitability to study the pharmacology of H_3R ligands. Therefore, we first stimulated these sensor cells with 10 µM of six reference H_3R ligands (histamine, imetit, UR-PI294, thioperamide, clobenpropit, pitolisant) that possess distinct intrinsic efficacies ranging from full agonism to inverse agonism (**Chart 1**, **Supplementary Table 1**). The BRET time-courses plateaued within several minutes after ligand addition and remained stable for at least 40 minutes (**Figure 3a**). The stability of the BRET response illustrates the broad time window for signal detection and underlines the applicability of this assay for automated screening conditions where stacked ligand-treated microtiter plates are read consecutively. Furthermore, all reference ligands yielded saturating BRET concentration-response curves and the EC_{50}-based order of potency resembled the pK_i-based order of affinity from our previous binding experiments (**Figure 3b**, **Supplementary Table 1**). For few ligands however, we obtained distinct affinities / potencies using the radioligand displacement assay in cell lysates or the BRET-based conformational readout in intact cells (e.g. for clobenpropit). Similar deviations have been reported recently for H_3R ligand affinities assessed in either radioligand displacement or NanoBRET binding experiments on the very same Nluc-tagged H_3R construct.[32] Therefore, we suppose that differences in assay conditions (e.g. buffer composition or receptor environment in intact cells vs. cell lysates) account for the few deviations observed in our experiments.

Of note, the three agonists histamine, imetit and UR-PI294 elevated the BRET ratio with distinct maximal effects (E_{max}). To the best of our knowledge, this is the first data indicating that imetit behaves as a strong partial rather than a full agonist at the receptor level. In contrast to the increase in BRET evoked by agonists, the H_3R inverse agonists thioperamide, clobenpropit and pitolisant induced a reduction in BRET, in line with their distinct downstream effects. However, surprisingly, thioperamide, clobenpropit and pitolisant plateaued at different BRET signals (E_{max} of pitolisant > clobenpropit > thioperamide), similar to the differences we observed for agonists, i.e. imetit and histamine. This suggests that also these ligands possess distinct inverse efficacies with pitolisant being the strongest inverse agonist.

Next, we aimed to explore whether Δicl3-$H_3R_{Nluc/Halo(618)}$ can be utilized to conduct structure-activity-relationship (SAR) studies with H_3R ligands. We selected a panel of three chemical analogues of the H_3R agonist impentamine that present distinct chemical substitutions at the amine group (**Chart 1**). When characterized at the second messenger cyclic adenosine monophosphate (cAMP) level, these ligands displayed varying efficacies ranging from strong partial agonism for impentamine to inverse agonism for VUF4903 (**Supplementary Table 1**).[28] The conformational H_3R sensor Δicl3-$H_3R_{Nluc/Halo(618)}$ detected these differential ligand activities and reported partial agonistic responses for the parent compound impentamine and its analogue VUF5207, as well as inverse agonistic responses with distinct E_{max} values for VUF4904 and VUF4903 (**Figure 3c**, **Supplementary Table 1**). Overall, these results demonstrate that Δicl3-$H_3R_{Nluc/Halo(618)}$ provides a valuable tool to conduct SAR studies of H_3R ligands at the level of receptor conformation.

Last, we aimed to evaluate the sensitivity and reproducibility of this sensor cell line to screen simultaneously H_3R agonists and inverse agonists in a single high-throughput campaign (i.e. without the requirement to pre-incubate the cells with competing H_3R ligands). Therefore, we measured the Z-factors for agonists and inverse agonists applying either histamine or pitolisant as positive controls, respectively.[33] The resulting average Z-factors were well above 0.5 (histamine: 0.58 ± 0.02; pitolisant: 0.72 ± 0.02; mean ± s.e.m.) and showed low interday variability (histamine: 4.6%; pitolisant: 5.6%; coefficient of variation) highlighting the substantial agonist and inverse agonist screening windows and the robustness of this conformational readout (**Figure 3d – f**, **Supplementary Figure 2**). These results underline the applicability of this conformational biosensor to screen for and to characterize novel H_3R ligands with varying intrinsic activities by using the same experimental setup.

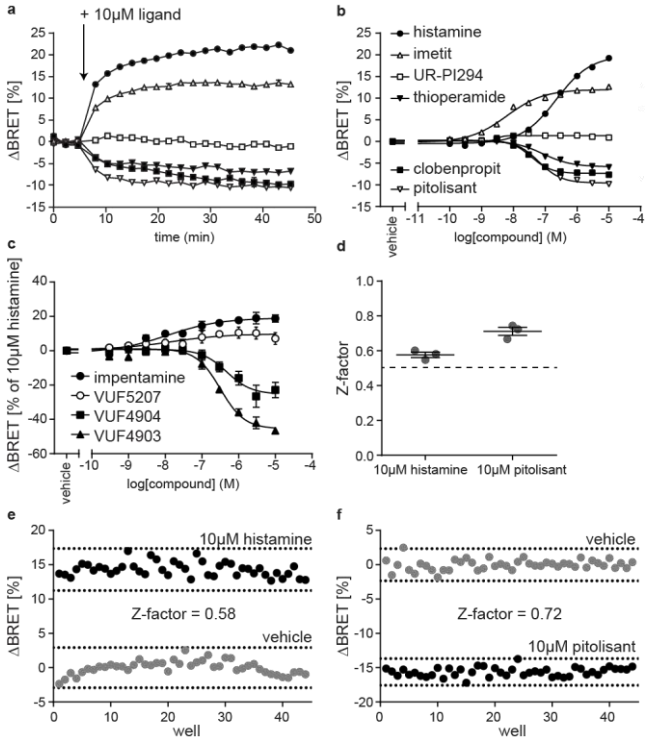

Figure 3. Validation of the Δicl3-$H_3R_{Nluc/Halo(618)}$ biosensor. a) ΔBRET time-course of six reference ligands (legend in b). b) BRET concentration-response curves of six reference ligands. c) Concentration-response curves of impentamine and three structural analogues. d) Z-factors of Δicl3-$H_3R_{Nluc/Halo(618)}$ to assess the screening windows for H_3R agonists and inverse agonists. e) BRET signals of one representative 96-well plate treated with 10 µM histamine or vehicle. f) BRET signals of one representative 96-well plate treated with 10 µM pitolisant or vehicle. All experiments were conducted in HEK293 cells stably expressing the Δicl3-$H_3R_{Nluc/Halo(618)}$ biosensor. Data in a - d show mean ± s.e.m. of at least three independent experiments.

Pharmacological characterization of two novel H_3R inverse agonists

To further demonstrate the ability of the conformational biosensor to characterize new H_3R targeting compounds, we used it to assess the pharmacological properties of two new H_3R ligands, Z27743747 and Z3303614736 (**Chart 1**). These compounds were discovered in a recent in-silico docking screen and validated for binding H_3R with nanomolar affinities.[26] However, further information on the pharmacological properties of Z27743747 and Z3303614736 is lacking, and this is hampering a reliable evaluation of their potential as novel H_3R modulating lead structures. We first incubated the stable H_3R biosensor cell line with 10 µM of either compound and in parallel conducted the same experiments using our previously described conformational biosensor of the β_2-adrenergic receptor ($\beta_2AR_{Nluc/Halo}$) [19]. Both ligands evoked fast and stable negative BRET changes in $H_3R_{Nluc/Halo}$ expressing cells but, as control, no BRET signals were observed in $\beta_2AR_{Nluc/Halo}$ (**Figure 4a**, **b**). Furthermore, application of increasing compound concentrations yielded sigmoidal concentration-response curves with nanomolar EC_{50}-values for $H_3R_{Nluc/Halo}$ but not $\beta_2AR_{Nluc/Halo}$ (**Figure 4c**, **4d**, **Supplementary Table 1**). Of note, Z27743747 evoked an even stronger BRET response than the reference inverse agonist pitolisant (**Supplementary Table 1**, **Supplementary Figure 3**), indicating that this ligand presents a promising chemical scaffold for the development of novel H_3R ligands with even greater intrinsic inverse agonistic activity.

To verify these data on a receptor downstream level, we employed a split luciferase complementation-based readout reflecting G-protein activity [34]. We co-expressed $G_{\alpha i1}$ and $G_{\beta 5}$ subunits tagged with complementary Nluc fragments along with native $G_{\gamma 2}$ and wildtype H_3R in HEK293 cells and pre-stimulated with 300 nM histamine to induce the dissociation of the heterotrimeric G-protein complex.

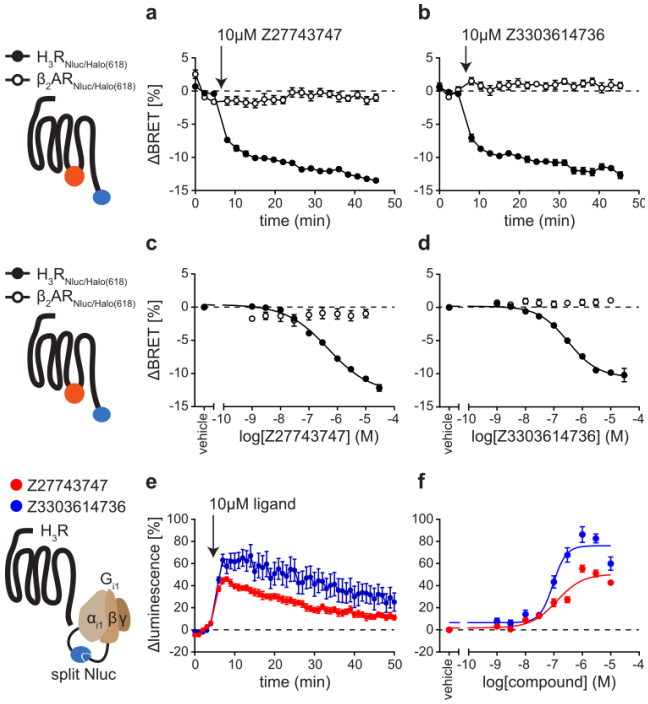

Figure 4. Characterization of new H_3R inverse agonists. a, b) ΔBRET time-course of Δicl3-$H_3R_{Nluc/Halo(618)}$ and $\beta_2AR_{Nluc/Halo(618)}$ upon addition of Z27743747 (a) and Z3303614736 (b). c, d) Concentration-response curves of Z27743747 (c) and Z3303614736 (d) applied to cells expressing Δicl3-$H_3R_{Nluc/Halo(618)}$ or $\beta_2AR_{Nluc/Halo(618)}$. e, f) ΔLuminescence time-course (e) and concentration-response (f) of the split Nluc-based G-protein sensor upon treatment with Z27743747 or Z3303614736. Experiments in a-d were conducted in HEK293 cells stably expressing either of the two conformational GPCR biosensors. Experiments in e and f were conducted in HEK293 cells transiently transfected with H_3R wildtype and the split Nluc-based G_{i1} sensor and pre-stimulated with 300 nM histamine (for 5 minutes before time point 0). Data show mean ± s.e.m. of at least three independent experiments.

Upon addition of 10 µM Z27743747 or Z3303614736, the luminescence intensity increased and peaked within several minutes, corresponding to a reassembly of the heterotrimeric G-protein complex (**Figure 4e**). Moreover, these signals were concentration-dependent and resulted in very similar IC_{50}-values as measured with the H_3R conformational biosensor (Z27743747: 6.90 ± 0.11; Z3303614736: 7.03 ± 0.07; pIC_{50} ± s.d.) (**Figure 4f**, **Supplementary Table 1**). Of note, only Z27743747, but not Z3303614736, was also able to induce an increase in G-protein luminescence when applied to basal H_3R (i.e. without 300 nM histamine pre-incubation) demonstrating its stronger inverse activity compared to Z3303614736 (**Supplementary Figure 4a**). However, the signal-to-noise ratio

(S/N) of this luminescence increase was substantially lower as compared to i) histamine pre-stimulated H_3R-G_i condition and ii) to the S/N ratio assessed with Δicl3-$H_3R_{Nluc/Halo(618)}$ (also without agonist pre-stimulation) (**Supplementary Figure 4b**).

Taken together, these results demonstrate that Z27743747 and Z3303614736 are new strong inverse agonists of the H_3R that inactivate the receptor with nanomolar potencies. Additionally, comparison of the different assay systems (Δicl3-$H_3R_{Nluc/Halo(618)}$ vs. H_3R wildtype plus G_{i1} sensor) underlines the accuracy and outstanding sensitivity of the new conformational H_3R biosensor to identify and characterize novel H_3R inverse agonist.

Conclusions

The histamine H_3 receptor is involved in multiple CNS disorders and rates among the most attractive and most targeted GPCRs by compounds in clinical trials.[35] Despite the extensive interest in regulating this receptor with new pharmaceutics, pitolisant represents so far the only approved H_3R targeting drug - partially due to the limitations of current H_3R-suited screening assays. In this work, we describe a new screening-compatible biosensor to aid in the future identification and pharmacological assessment of H_3R modulating compounds.

The novel H_3R conformational biosensor allows for the synchronous screening of agonists and inverse agonists

This new biosensor is composed of the BRET partners Nluc and a red fluorescent HaloTag dye fused to H_3R in order to translate the ligand-induced conformational dynamics of this receptor into optical signals.

We show that this sensor maintains wildtype-like ligand binding properties and facilitates the assessment of ligand potency and efficacy at the most proximal level, i.e. directly after ligand binding. Consequently, we were able to detect differences in ligand efficacies between the two H_3R agonists histamine and imetit, as well as between the inverse agonists thioperamide, clobenpropit and pitolisant (**Supplementary Table 1**). These distinct intrinsic activities could not be observed in previous studies using the FRET-based conformational H_3R sensor[23] or downstream-dependent H_3R assays[36] which might be a consequence of differential sensitivities of FRET- vs. BRET-based sensors[37] or, with respect to histamine and imetit, be due to the impact of signal amplification in downstream-dependent assays. Supporting this hypothesis, similar discrepancies between ligand efficacies assessed with FRET vs. BRET conformational sensors (UK 14,304 response at $\alpha_{2A}AR_{CFP/Flash}$ vs. $\alpha_{2A}AR_{Nluc/Halo(618)}$)[19, 38] and downstream vs. receptor conformation assays have been reported for the α_{2A}-adrenergic (norepinephrine vs. UK 14,304) and β_2-adrenergic receptor (epinephrine vs. norepinephrine).[19-21] Our findings with the H_3R conformational biosensor underline the superior resolution provided by conformational GPCR sensors for the determination of ligand efficacies.

Furthermore, we demonstrate that the H_3R biosensor can be employed to explore structure-activity relationships and provides excellent sensitivity and robustness for the simultaneous screening of H_3R agonists and inverse agonists. This feature is of great value in GPCR-targeted ligand screening campaigns since, in contrast to downstream-dependent assays, no pre-incubation with (or subsequent addition of) an H_3R agonists is required to identify inverse agonists or vice versa.

To the best of our knowledge, such a screening-compatible and uniform assay format is not provided by any other GPCR screening technology available today.

Characterization of novel H_3R ligands with marked inverse agonistic efficacy

In the last part of this study, we employed the novel H_3R conformational sensor to assess the pharmacological properties of two new H_3R ligands that were recently discovered through virtual screening.[26] Both compounds bind H_3R with nanomolar affinity, but their intrinsic efficacies have not been determined so far. Interestingly, our results with the H_3R conformational biosensor revealed pronounced inverse agonistic responses of the ligands Z27743747 and Z3303614736. In particular Z27743747 induced even higher BRET amplitudes than the validated inverse agonists thioperamide, clobenpropit and pitolisant. This suggests that Z27743747 presents stronger inverse agonistic activity than the current gold standard pitolisant (**Supplementary Table 1**, **Supplementary Figure 3**) by stabilizing a distinct conformation of H_3R that is characterized by no or very little residual receptor signalling capacity.

Therefore, Z27743747 and Z3303614736 represent two promising H_3R lead structures with novel chemical scaffolds that can serve for the design of superior H_3R ligands with advantageous pharmacodynamic properties.

Taken together, this work describes the successful generation of the first screening applicable H_3R conformational sensor. This optical tool will aid in the development of novel receptor ligands and may be employed to gain new insights into the molecular mechanisms underlying H_3R conformational dynamics. The successful implementation of this sensor design for the H_3R opens up the possibility to expand this technique to other class A GPCRs, e.g. the other members of the histamine receptor family, to assess the pharmacological properties of GPCR ligands directly at the level of receptor conformation.

ASSOCIATED CONTENT

Supporting Information.
The supporting information is available free of charge via the Internet at http://pubs.acs.org. Supplementary Table 1; Supplementary Figures 1 – 4

AUTHOR INFORMATION

Corresponding Authors

Hannes Schihada - Section of Receptor Biology & Signaling, Dept. Physiology & Pharmacology, Karolinska Institutet, Stockholm, Sweden; Email: hannes.schihada@ki.se

Martin J. Lohse – Institute of Pharmacology and Toxicology and Rudolf Virchow Center, University of Würzburg, Würzburg, Germany; Email: m.lohse@mdc.de

Author Contributions

The manuscript was written through contributions of all authors. All authors have given approval to the final version of the manuscript.

Funding Sources

This work was supported by the National Institutes of Health (NIH, 0255-8521-4609), by SFB/TR166 and by the Bundesministerium für Bildung und Forschung (BMBF, Federal Ministry of Education and Research - OptiMAR) to M.J.L. and by the Deutsche Forschungsgemeinschaft (DFG, German Research Foundation – 427840891) to H.S. The work at Karolinska Insti-

tutet was supported by grants from Karolinska Institutet, the Swedish Research Council (2017-04676) and the Swedish Cancer Society (CAN2017/561). The work at Vrije Universiteit was supported by a CSC Chinese scholarship grant to X.M.

Notes

The authors declare that The University of Würzburg holds a patent on this technology: WO2004057333 A1.

ACKNOWLEDGMENT

We thank Kristina Lorenz (University of Wuerzburg, Germany) and Anna Krook (Karolinska Institutet, Sweden) for access to the Synergy Neo2 and ClarioStar plate reader, respectively. Furthermore, we thank Asuka Inoue (Tohoku University, Japan) for providing plasmids encoding the G-protein sensor.

ABBREVIATIONS

GPCR, G-protein-coupled receptor; H_3R, histamine H_3 receptor; CNS, central nervous system; FRET, fluorescence resonance energy transfer; BRET, bioluminescence resonance energy transfer; icl3, intracellular loop three; [^{3}H]NAMH, N-α-methylhistamine; SAR, structure-activity-relationship; S/N ratio, signal-to-noise ratio.

REFERENCES

1. Panula, P.; Chazot, P. L.; Cowart, M.; Gutzmer, R.; Leurs, R.; Liu, W. L.; Stark, H.; Thurmond, R. L.; Haas, H. L., International Union of Basic and Clinical Pharmacology. XCVIII. Histamine Receptors. Pharmacol Rev 2015, 67 (3), 601-655.
2. Bradshaw, J.; Brittain, R. T.; Clitherow, J. W.; Daly, M. J.; Jack, D.; Price, B. J.; Stables, R., Ranitidine (AH 19065): a new potent, selective histamine H2-receptor antagonist [proceedings]. Br J Pharmacol 1979, 66 (3), 464-464.
3. Barnett, A.; Iorio, L. C.; Kreutner, W.; Tozzi, S.; Ahn, H. S.; Gulbenkian, A., Evaluation of the CNS properties of SCH 29851, a potential non-sedating antihistamine. Agents Actions 1984, 14 (5-6), 590-597.
4. Arrang, J. M.; Garbarg, M.; Schwartz, J. C., Auto-inhibition of brain histamine release mediated by a novel class (H3) of histamine receptor. Nature 1983, 302 (5911), 832-837.
5. Nieto-Alamilla, G.; Marquez-Gomez, R.; Garcia-Galvez, A. M.; Morales-Figueroa, G. E.; Arias-Montano, J. A., The Histamine H3 Receptor: Structure, Pharmacology, and Function. Mol Pharmacol 2016, 90 (5), 649-673.
6. Ferrada, C.; Ferre, S.; Casado, V.; Cortes, A.; Justinova, Z.; Barnes, C.; Canela, E. I.; Goldberg, S. R.; Leurs, R.; Lluis, C.; Franco, R., Interactions between histamine H3 and dopamine D2 receptors and the implications for striatal function. Neuropharmacology 2008, 55 (2), 190-197.
7. Rodriguez-Ruiz, M.; Moreno, E.; Moreno-Delgado, D.; Navarro, G.; Mallol, J.; Cortes, A.; Lluis, C.; Canela, E. I.; Casado, V.; McCormick, P. J.; Franco, R., Heteroreceptor Complexes Formed by Dopamine D1, Histamine H3, and N-Methyl-D-Aspartate Glutamate Receptors as Targets to Prevent Neuronal Death in Alzheimer's Disease. Mol Neurobiol 2017, 54 (6), 4537-4550.
8. Rapanelli, M., The magnificent two: histamine and the H3 receptor as key modulators of striatal circuitry. Prog Neuropsychopharmacol Biol Psychiatry 2017, 73, 36-40.
9. Rapanelli, M.; Frick, L.; Pogorelov, V.; Ohtsu, H.; Bito, H.; Pittenger, C., Histamine H3R receptor activation in the dorsal striatum triggers stereotypies in a mouse model of tic disorders. Transl Psychiatry 2017, 7 (1), e1013, https://doi.org/10.1038/tp.2016.290
10. Syed, Y. Y., Pitolisant: First Global Approval. Drugs 2016, 76 (13), 1313-1318.
11. Wagner, G.; Mocking, T. A. M.; Arimont, M.; Provensi, G.; Rani, B.; Silva-Marques, B.; Latacz, G.; Da Costa Pereira, D.; Karatzidou, C.; Vischer, H. F.; Wijtmans, M.; Kiec-Kononowicz, K.; de Esch, I. J. P.; Leurs, R., 4-(3-Aminoazetidin-1-yl)pyrimidin-2-amines as High-Affinity Non-imidazole Histamine H3 Receptor Agonists with in Vivo Central Nervous System Activity. J Med Chem 2019, 62 (23), 10848-10866.
12. Wagner, G.; Mocking, T. A. M.; Kooistra, A. J.; Slynko, I.; Abranyi-Balogh, P.; Keseru, G. M.; Wijtmans, M.; Vischer, H. F.; de Esch, I. J. P.; Leurs, R., Covalent Inhibition of the Histamine H3 Receptor. Molecules 2019, 24 (24), doi: 10.3390/molecules24244541.
13. Hauwert, N. J.; Mocking, T. A. M.; Da Costa Pereira, D.; Lion, K.; Huppelschoten, Y.; Vischer, H. F.; De Esch, I. J. P.; Wijtmans, M.; Leurs, R., A Photoswitchable Agonist for the Histamine H3 Receptor, a Prototypic Family A G-Protein-Coupled Receptor. Angew Chem Int Ed Engl 2019, 58 (14), 4531-4535.
14. Darras, F. H.; Pockes, S.; Huang, G.; Wehle, S.; Strasser, A.; Wittmann, H. J.; Nimczick, M.; Sotriffer, C. A.; Decker, M., Synthesis, biological evaluation, and computational studies of Tri- and tetracyclic nitrogen-bridgehead compounds as potent dual-acting AChE inhibitors and hH3 receptor antagonists. ACS Chem Neurosci 2014, 5 (3), 225-242.
15. Ghamari, N.; Dastmalchi, S.; Zarei, O.; Arias-Montano, J. A.; Reiner, D.; Ustun-Alkan, F.; Stark, H.; Hamzeh-Mivehroud, M., In silico and in vitro studies of two non-imidazole multiple targeting agents at histamine H3 receptors and cholinesterase enzymes. Chem Biol Drug Des 2019, doi: 10.1111/cbdd.13642.
16. Lutsenko, K.; Hagenow, S.; Affini, A.; Reiner, D.; Stark, H., Rasagiline derivatives combined with histamine H3 receptor properties. Bioorg Med Chem Lett 2019, 29 (19), 126612, doi: 10.1016/j.bmcl.2019.08.016.
17. Lazewska, D.; Kiec-Kononowicz, K., Progress in the development of histamine H3 receptor antagonists/inverse agonists: a patent review (2013-2017). Expert opinion on therapeutic patents 2018, 28 (3), 175-196.
18. Lohse, M. J.; Nuber, S.; Hoffmann, C., Fluorescence/bioluminescence resonance energy transfer techniques to study G-protein-coupled receptor activation and signaling. Pharmacol Rev 2012, 64 (2), 299-336.
19. Schihada, H.; Vandenabeele, S.; Zabel, U.; Frank, M.; Lohse, M. J.; Maiellaro, I., A universal bioluminescence resonance energy transfer sensor design enables high-sensitivity screening of GPCR activation dynamics. Commun Biol 2018, 1, 105, doi: 10.1038/s42003-018-0072-0.
20. Reiner, S.; Ambrosio, M.; Hoffmann, C.; Lohse, M. J., Differential signaling of the endogenous agonists at the beta2-adrenergic receptor. J Biol Chem 2010, 285 (46), 36188-36198.
21. Liu, J. J.; Horst, R.; Katritch, V.; Stevens, R. C.; Wuthrich, K., Biased signaling pathways in beta2-adrenergic receptor characterized by 19F-NMR. Science 2012, 335 (6072), 1106-1110.
22. Erdogmus, S.; Storch, U.; Danner, L.; Becker, J.; Winter, M.; Ziegler, N.; Wirth, A.; Offermanns, S.; Hoffmann, C.; Gudermann, T.; Mederos, Y. S. M., Helix 8 is the essential structural motif of mechanosensitive GPCRs. Nat Commun 2019, 10 (1), 5784, doi: 10.1038/s41467-019-13722-0.
23. Liu, Y.; Zeng, H.; Pediani, J. D.; Ward, R. J.; Chen, L. Y.; Wu, N.; Ma, L.; Tang, M.; Yang, Y.; An, S.; Guo, X. X.; Hao, Q.; Xu, T. R., Visualization of the activation of the histamine H3 receptor (H3R) using novel fluorescence resonance energy transfer biosensors and their potential application to the study of H3R pharmacology. FEBS J 2018, 285 (12), 2319-2336.
24. Hall, M. P.; Unch, J.; Binkowski, B. F.; Valley, M. P.; Butler, B. L.; Wood, M. G.; Otto, P.; Zimmerman, K.; Vidugiris, G.; Machleidt, T.; Robers, M. B.; Benink, H. A.; Eggers, C. T.;

Slater, M. R.; Meisenheimer, P. L.; Klaubert, D. H.; Fan, F.; Encell, L. P.; Wood, K. V., Engineered luciferase reporter from a deep sea shrimp utilizing a novel imidazopyrazinone substrate. ACS Chem Biol 2012, 7 (11), 1848-1857.
25. Los, G. V.; Encell, L. P.; McDougall, M. G.; Hartzell, D. D.; Karassina, N.; Zimprich, C.; Wood, M. G.; Learish, R.; Ohana, R. F.; Urh, M.; Simpson, D.; Mendez, J.; Zimmerman, K.; Otto, P.; Vidugiris, G.; Zhu, J.; Darzins, A.; Klaubert, D. H.; Bulleit, R. F.; Wood, K. V., HaloTag: a novel protein labeling technology for cell imaging and protein analysis. ACS Chem Biol 2008, 3 (6), 373-382.
26. Schaller, D.; Hagenow, S.; Stark, H.; Wolber, G., Ligand-guided homology modeling drives identification of novel histamine H3 receptor ligands. PLoS One 2019, 14 (6), e0218820, doi: 10.1371/journal.pone.0218820.
27. Igel, P.; Schnell, D.; Bernhardt, G.; Seifert, R.; Buschauer, A., Tritium-labeled N(1)-[3-(1H-imidazol-4-yl)propyl]-N(2)-propionylguanidine ([(3)H]UR-PI294), a high-affinity histamine H(3) and H(4) receptor radioligand. ChemMedChem 2009, 4 (2), 225-231.
28. Wieland, K.; Bongers, G.; Yamamoto, Y.; Hashimoto, T.; Yamatodani, A.; Menge, W. M.; Timmerman, H.; Lovenberg, T. W.; Leurs, R., Constitutive activity of histamine h(3) receptors stably expressed in SK-N-MC cells: display of agonism and inverse agonism by H(3) antagonists. J Pharmacol Exp Ther 2001, 299 (3), 908-914.
29. Vilardaga, J. P.; Bunemann, M.; Krasel, C.; Castro, M.; Lohse, M. J., Measurement of the millisecond activation switch of G protein-coupled receptors in living cells. Nat Biotechnol 2003, 21 (7), 807-812.
30. Hoffmann, C.; Gaietta, G.; Bunemann, M.; Adams, S. R.; Oberdorff-Maass, S.; Behr, B.; Vilardaga, J. P.; Tsien, R. Y.; Ellisman, M. H.; Lohse, M. J., A FlAsH-based FRET approach to determine G protein-coupled receptor activation in living cells. Nat Methods 2005, 2 (3), 171-176.
31. Kauk, M.; Hoffmann, C., Intramolecular and Intermolecular FRET Sensors for GPCRs - Monitoring Conformational Changes and Beyond. Trends Pharmacol Sci 2018, 39 (2), 123-135.
32. Mocking, T. A. M.; Verweij, E. W. E.; Vischer, H. F.; Leurs, R., Homogeneous, Real-Time NanoBRET Binding Assays for the Histamine H3 and H4 Receptors on Living Cells. Mol Pharmacol 2018, 94 (6), 1371-1381.
33. Zhang, J. H.; Chung, T. D.; Oldenburg, K. R., A Simple Statistical Parameter for Use in Evaluation and Validation of High Throughput Screening Assays. J Biomol Screen 1999, 4 (2), 67-73.
34. Inoue, A.; Raimondi, F.; Kadji, F. M. N.; Singh, G.; Kishi, T.; Uwamizu, A.; Ono, Y.; Shinjo, Y.; Ishida, S.; Arang, N.; Kawakami, K.; Gutkind, J. S.; Aoki, J.; Russell, R. B., Illuminating G-Protein-Coupling Selectivity of GPCRs. Cell 2019, 177 (7), 1933-1947 e1925.
35. Hauser, A. S.; Attwood, M. M.; Rask-Andersen, M.; Schioth, H. B.; Gloriam, D. E., Trends in GPCR drug discovery: new agents, targets and indications. Nature reviews. Drug discovery 2017, 16 (12), 829-842.
36. Lim, H. D.; van Rijn, R. M.; Ling, P.; Bakker, R. A.; Thurmond, R. L.; Leurs, R., Evaluation of histamine H1-, H2-, and H3-receptor ligands at the human histamine H4 receptor: identification of 4-methylhistamine as the first potent and selective H4 receptor agonist. J Pharmacol Exp Ther 2005, 314 (3), 1310-1321.
37. Boute, N.; Jockers, R.; Issad, T., The use of resonance energy transfer in high-throughput screening: BRET versus FRET. Trends Pharmacol Sci 2002, 23 (8), 351-354.
38. Nikolaev, V. O.; Hoffmann, C.; Bunemann, M.; Lohse, M. J.; Vilardaga, J. P., Molecular basis of partial agonism at the neurotransmitter alpha2A-adrenergic receptor and Gi-protein heterotrimer. J Biol Chem 2006, 281 (34), 24506-24511.

Table of Contents artwork (for TOC only)